Drug Development and Industrial Pharmacy

ISSN: (Print) (Online) Journal homepage: https://www.tandfonline.com/loi/iddi20

Impact of the functional coating of silver nanoparticles on their *in vivo* performance and biosafety

Hesham M. Tawfeek, Mahmoud A. Younis, Basmah Nasser Aldosari, Alanood Sunhat Almurshedi, Ahmed Abdelfattah & Jelan A. Abdel-Aleem

To cite this article: Hesham M. Tawfeek, Mahmoud A. Younis, Basmah Nasser Aldosari, Alanood Sunhat Almurshedi, Ahmed Abdelfattah & Jelan A. Abdel-Aleem (2023) Impact of the functional coating of silver nanoparticles on their *in vivo* performance and biosafety, Drug Development and Industrial Pharmacy, 49:5, 349-356, DOI: 10.1080/03639045.2023.2214207

To link to this article: https://doi.org/10.1080/03639045.2023.2214207

Published online: 27 May 2023.

DRUG DEVELOPMENT AND INDUSTRIAL PHARMACY
2023, VOL. 49, NO. 5, 349–356
https://doi.org/10.1080/03639045.2023.2214207

Taylor & Francis
Taylor & Francis Group

RESEARCH ARTICLE

Impact of the functional coating of silver nanoparticles on their *in vivo* performance and biosafety

Hesham M. Tawfeek[a], Mahmoud A. Younis[a], Basmah Nasser Aldosari[b], Alanood Sunhat Almurshedi[b], Ahmed Abdelfattah[a#] and Jelan A. Abdel-Aleem[a]

[a]Department of Industrial Pharmacy, Faculty of Pharmacy, Assiut University, Assiut, Egypt; [b]Department of Pharmaceutics, College of Pharmacy, King Saud University, Riyadh, Saudi Arabia

ABSTRACT

Objective and significance: Silver nanoparticles (AgNPs) have become an interesting therapeutic modality and drug delivery platform. Herein, we aimed to investigate the impact of functional coating on the *in vivo* performance of AgNPs as an economic and scalable method to modulate their behavior.

Methods: AgNPs were coated with chitosan (CHI) as a model biopolymer using a one-pot reduction-based method, where CHI of two molecular weight ranges were investigated. The resultant CHI-coated AgNPs (AgNPs-CHI) were characterized using UV-VIS spectroscopy, DLS, and TEM. AgNPs were administered intravenously to rats and their biodistribution and serum levels of hepato-renal function markers were monitored 24 h later compared to plain $AgNO_3$ as a positive control.

Results: UV-VIS spectroscopy confirmed the successful coating of AgNPs with CHI. DLS revealed the superiority of medium molecular weight CHI over its low molecular weight counterpart. AgNPs-CHI demonstrated a semi-complete clearance from the systemic circulation, a liver-dominated tissue tropism, and limited renal exposure. On the other hand, $AgNO_3$ was poorly cleared from the circulation, with relatively high renal exposure and a non-specific tissue tropism. AgNPs-CHI were well-tolerated by the liver and kidney without signs of toxicity or inflammation, in contrary with $AgNO_3$ which resulted in a significant elevation of Creatinine (CRE), Urea, and Total Protein (TP), suggesting a significant nephrotoxicity and inflammation.

Conclusions: Functional coating of AgNPs with CHI substantially modulated their *in vivo* behavior, promoting their hepatic selectivity and biotolerability, which can be invested in the development of drug delivery systems for the treatment of liver diseases.

ARTICLE HISTORY
Received 18 March 2023
Revised 4 May 2023
Accepted 10 May 2023

KEYWORDS
Silver nanoparticles; functional coating; chitosan; biodistribution; biosafety

Introduction

Nanomedicines have witnessed a breakthrough recently with an increasing focus on their clinical translation, aiming at the development of clinically-relevant products for the treatment of various human disorders [1,2]. While an extensive focus has been directed to lipid nanoparticles (LNPs), inspired by the massive advancements in the development of gene therapies and vaccines [3–5], limited interest has been given to inorganic nanoparticles in spite of their attractive features including ease of fabrication, scalability, and high stability [6]. Silver nanoparticles (AgNPs) are an interesting subclass of inorganic nanoparticles, with versatile applicability and several attractive features such as their antimicrobial and wound-healing properties [7,8]. In addition, AgNPs can be used as drug delivery nanocarriers and/or theranostic agents owing to their excellent optical properties, *ex vivo* and *in vivo* stability, and high drug loading capacity [9]. Nevertheless, the concerns about the biosafety of AgNPs in addition to their lack of selectivity and poor body clearability have limited their widespread *in vivo* application and clinical trials [10], which left the pharmaceutical market deprived of the outstanding benefits of such a platform. Therefore, innovative solutions are essential to bring this technology to the market in a more efficient and reliable way.

Functional coating of inorganic nanoparticles is a promising strategy to modulate their *in vivo* performance, biodistribution, clearance, and biosafety. A wide variety of biopolymers were investigated as functional coatings such as poly(ethylene glycol) (PEG), cellulose, sodium alginate, and poly(vinyl pyrrolidone) (PVP) [9,11–13]. Furthermore, the functional coating can be a more clinically-translatable approach in terms of scalability in comparison with the classic ligand-based targeting. Chitosan (CHI) is a carbohydrate-based polymer of N-acetyl-D-glucosamine, synthesized *via* the deacetylation of the naturally-occurring polymer, chitin. Thanks to its attractive features including ease of synthesis, ease of chemical modification, flexibility, and high tolerability, CHI has been investigated in a wide diversity of drug delivery applications [14]. Moreover, the biodegradability of chitosan has prompted its use as a biosafe polymeric coating in several drug delivery platforms [15]. Furthermore, numerous recent studies revealed some interesting biological activities of CHI including hypocholesterolemic, antimicrobial, immunostimulant, antioxidant, anti-inflammatory, and anticancer effects [16–18].

In the present study, we selected CHI as a model biopolymer for the functional coating of AgNPs aiming at exploring the impact of such a coating on the *in vivo* performance and biosafety

CONTACT Hesham M. Tawfeek heshamtawfeek@aun.edu.eg; Mahmoud A. Younis mahmoudyounis@aun.edu.eg Department of Industrial Pharmacy, Faculty of Pharmacy, Assiut University, Assiut, 71526, Egypt
#Faculty of Pharmacy and Pharmaceutical Sciences, University of Alberta, Edmonton, AB T6G 2E1, Canada.

of AgNPs. First, CHI of two molecular weight ranges were investigated to select the optimum biopolymer for an efficient and stable coating. Then, the *in vivo* biodistribution to the various tissues was investigated in rats post intravenous administration using Inductively Coupled Plasma Mass Spectrometry (ICP-MS). Moreover, the impact of such a coating on the *in vivo* biosafety of AgNPs was explored *via* the post-administration serum analysis of hepato-renal function markers; Aspartate transaminase (AST), Alanine aminotransferase (ALT), Creatinine (CRE), Urea, and Total Protein (TP).

Material and methods

Materials

Chitosan polymers with a low molecular weight (50–190 KDa) and a medium molecular weight (190–310 KDa), as well as commercial kits for the assay of AST, ALT, CRE, and Urea, were obtained from Sigma Aldrich, USA. Sodium borohydride ($NaBH_4$) was purchased from S D Fine-Chem Limited (India). Silver nitrate ($AgNO_3$) was purchased from Alpha Chemicals (Cairo, Egypt). Glacial acetic acid was obtained from Sigma Aldrich, Egypt. Pierce™ Bicinchoninic Acid (BCA) Protein Assay Kit and sterile Phosphate Buffer Saline Solution, PBS (−), were purchased from Thermofisher Scientific, USA. All other used chemicals and reagents were of analytical grade and were used without further processing.

Animals

Seven-week-old Male Sprague–Dawley rats (average body weight = 200–250 g) were obtained from Assiut University Animal House (Assiut, Egypt) and were handled according to the ethical guidelines for handling laboratory animals. The animals were fed a standard pelleted diet containing 5% fibers, 20% protein, and 5–10% fat, and had free access to food and water during the experiments. All the experimental protocols were approved by the Assiut University Ethics Committee (Faculty of Pharmacy, Assiut University, local approval number 17300885, date of original approval: 25/10/2022).

Preparation of and characterization of AgNPs-CHI

AgNPs-CHI were fabricated using a simultaneous one-pot coating/redox reaction as described previously [19]. Two ranges of molecular weights for the coating polymer were screened; namely a low molecular weight range (50–190 KDa) and a medium molecular weight range (190–310 KDa). Figure 1 outlines the scheme that was adopted in the preparation. Briefly, fifty milligrams of the investigated polymer were dissolved in 10 ml of an aqueous solution of glacial acetic acid (10% v/v), followed by mixing with 5 ml of an aqueous solution of $AgNO_3$ (1 mM). The reaction mixture was then diluted to 100 ml with double-distilled water under continuous stirring in an ice bath for 10 min. Sixty microliters of $NaBH_4$ (0.1 M) were added in a dropwise manner to reduce the $AgNO_3$ precursor into the corresponding AgNPs, under continuous stirring for 45–60 min to facilitate the completion of the reaction. The final mixture was maintained in room temperature under stirring for an extra 15–30 min prior to centrifugation to retrieve the resultant AgNPs-CHI, which were further dispersed in an isotonic solution of PBS (−) that is suitable for the *in vivo* experiments.

UV-VIS spectroscopy was performed to prove the formation of coated AgNPs. AgNPs prepared *via* reduction using sodium borohydride and the formulated AgNPs-CHI solutions were scanned from 300 to 600 nm using a double-beam spectrophotometer (PerkinElmer, lambda25 UV–Vis Spectrophotometer) [20]. In addition, AgNPs-CHI were characterized using Dynamic Light Scattering (DLS) in a Zetasizer Nano ZS analyzer (Malvern Instruments, UK) as reported previously [21,22]. Furthermore, the morphology and structure of AgNPs-CHI were examined by Transmission Electron Microscopy (TEM). A sample of 10 µL of AgNPs-CHI solution was applied to a double-sided copper grid (Nisshin EM Co., Japan) and air-dried overnight. Images were captured using a transmission electron microscope (JEM-1230, JEOL, Japan) using a magnification power of 5000–10,000× and under an accelerating voltage of 100 KV.

In vivo *biodistribution study*

The rats were randomly divided into two groups ($n = 5$) and injected intravenously with AgNPs-CHI (10 mg/Kg) or $AgNO_3$

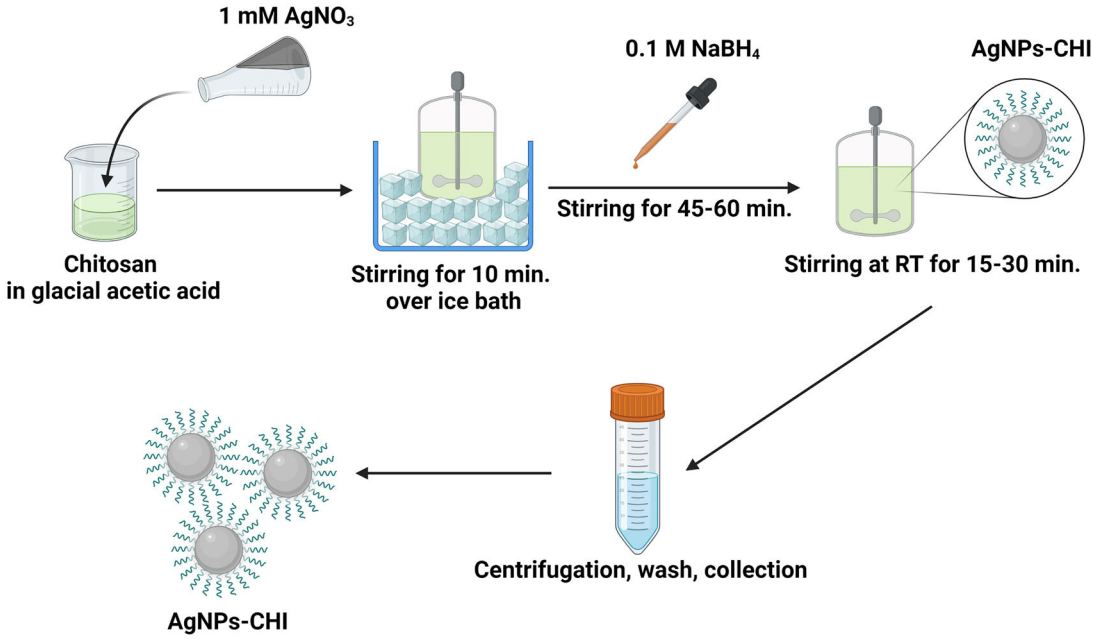

Figure 1. A scheme outlining the preparation steps of AgNPs-CHI. The figure was created with BioRender.com software, with a publication license.

solution (17 mg/Kg). The dose of $AgNO_3$ was adjusted to result in an equivalent silver content to that for AgNPs-CHI and was used as a positive control to reflect the behavior of the plain silver. The animals were euthanized by cervical dislocation 24 h post-administration, according to the guidelines of the American Veterinary Medical Association (AVMA) [23], and the major organs as well as blood were collected for analysis. The amount of silver per one gram of the homogenized tissues or 1 ml of blood was determined by Inductively Coupled Plasma Mass Spectrometry (ICP-MS) as reported previously [24,25].

Evaluation of the biosafety

Blood samples from rats that were injected with AgNPs-CHI or $AgNO_3$ were collected from the Vena Cava 24 h post administration at the doses specified above. Blood was allowed to clot for 4 h at 4 °C prior to centrifugation at 1200 g, 4 °C, for 30 min to separate the serum that was kept at −80 °C until analysis [26,27]. The serum levels of the hepato-renal function markers; AST, ALT, CRE, and Urea were determined using commercially-available kits according to the manufacturer's guidelines. Total Protein (TP) in serum was determined by BCA assay as described previously [28]. The results were compared to the values for negative control rats that were treated with PBS (−) under the same experimental conditions.

Statistical analysis

Statistical analyses and data plotting were performed using Graphpad Prism 8 software. Two-way Analysis of Variance (ANOVA) followed by the Bonferroni test were used for multiple comparisons in two-factor experiments. *p*-value <.05 was considered to be significant.

Results

The formation of AgNPs was monitored thanks to the characteristic yellow color that started to appear 15 min post addition of $NaBH_4$ to the reaction medium. UV VIS spectroscopy showed the characteristic surface plasmon effect with a maximum absorption band at λ_{max} of 405 and 394 nm for AgNPs-CHI and uncoated AgNPs, respectively, as shown in Figure 2.

CHI of two different molecular weight ranges was used as a functional coating for AgNPs and the physicochemical characteristics of the resultant nanosystems were studied by DLS. AgNPs that were coated with a low molecular weight CHI demonstrated large hydrodynamic diameters (>600 nm) and low zeta potential (<10 mV). In contrast, AgNPs that were coated with a medium molecular weight CHI showed acceptable hydrodynamic diameters (~280 nm) and a highly-positive zeta potential (~50 mV). Therefore, the latter candidate was selected and the resultant AgNPs were referred to as AgNPs-CHI in the subsequent sections of this study. AgNPs-CHI were further examined by TEM, where the micrographs revealed spherical monodisperse particles with a solid metallic core of approximately 20 nm (Figure 3).

The *in vivo* biodistribution of AgNPs-CHI was investigated following intravenous administration to rats, where systemic intravenous administration was adopted for better clinical relevance. A solution of plain $AgNO_3$ was used as a positive control to represent the *in vivo* behavior of the plain silver. Figure 4 shows the biodistribution in the major organs and blood 24 h post-administration. Interestingly, a substantial proportion of the recovered

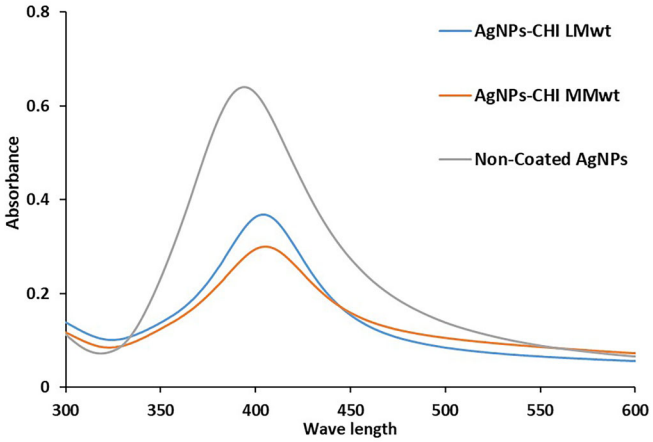

Figure 2. UV-VIS spectroscopy of CHI-coated AgNPs (AgNPs-CHI) and non-coated AgNPs. Abbreviations: LMwt, Low molecular weight; MMwt, Medium molecular weight.

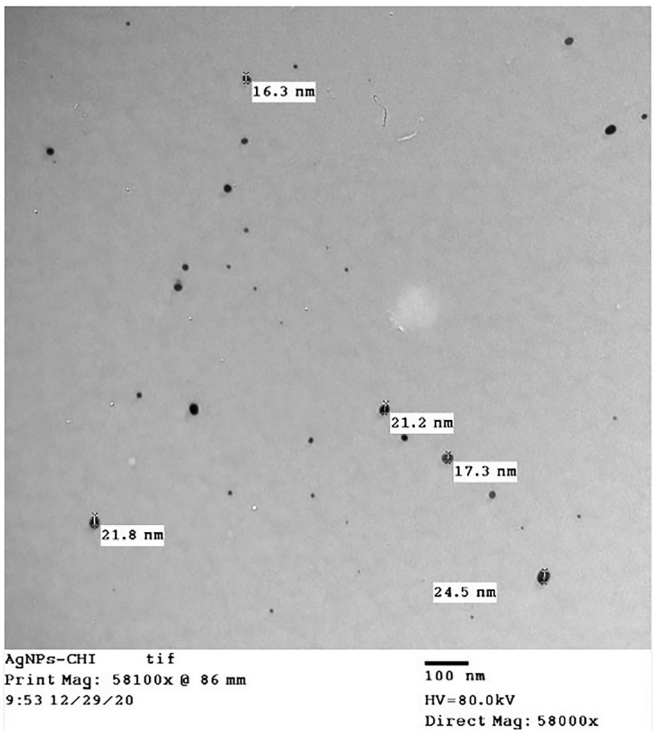

Figure 3. Transmission electron microscope image of AgNPs-CHI MMwt. Scale bar represents 100 nm and magnification of 58,000×.Image shows the size of the produced AgNPs-CHI, with a mean diameter of 20.22 ± 3.3 nm.

silver (more than 40%) was retrieved from the blood of the rats in the case of the plain $AgNO_3$, where the liver cleared only about 20% of the silver amount. In addition, plain silver demonstrated nonspecific accumulations in the liver, spleen, kidneys, and lungs. On the contrary, functional coating of the silver with CHI dramatically changed its *in vivo* behavior, where approximately 70% of the silver amount were recovered from the liver indicating an obvious hepatic selectivity. Meanwhile, the blood level of the silver in the case of AgNPs-CHI was approximately 5%, which indicated a good capability of the body to clear the CHI-coated nanosilver from the systemic circulation following its intravenous administration. It is also noteworthy that the amount of the recovered silver in the kidneys of AgNPs-CHI-treated rats was half of its value in the case of $AgNO_3$-treated rats.

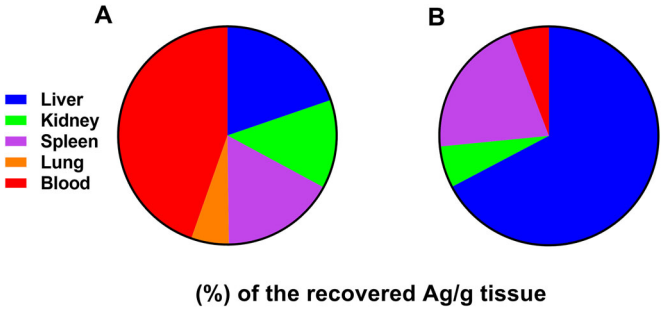

Figure 4. The *in vivo* biodistribution of plain $AgNO_3$ solution (A) in comparison with the prepared AgNPs-CHI (B) 24 h post intravenous administration to rats. The amount of silver in each organ was quantified by ICP-MS and presented as (%) of the total recovered silver (Ag) per 1 g of tissues. To facilitate easier comparisons, the blood density was rounded to 1 g/mL and the (%) of the total recovered Ag per 1 ml blood was presented similarly. The average of $N = 5$ was considered in the calculations.

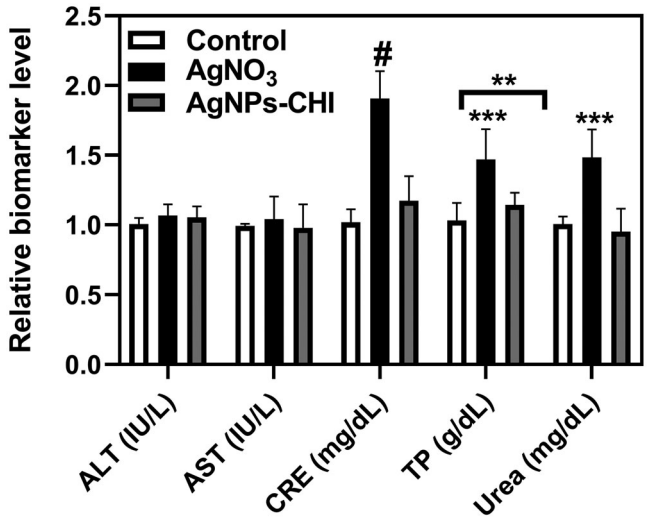

Figure 5. The *in vivo* biosafety of AgNPs-CHI in comparison with plain $AgNO_3$ (positive control) or PBS solutions (negative control) 24 h post intravenous administration to rats in doses equivalent to 10 mg/Kg and 17 mg/Kg for AgNPs-CHI and $AgNO_3$, respectively. The serum levels of the investigated biomarkers were expressed relative to the normal values for the negative control groups. $N = 5$, average ± standard deviation. #$p < .0001$ versus the control and AgNPs-CHI groups, ** $p < .01$, *** $p < .001$ for TP in case of $AgNO_3$ versus the control group and for Urea in $AgNO_3$-treated rats versus the control and AgNPs-CHI groups.

To assess the impact of functional coating by CHI on the *in vivo* biosafety of the nanosilver, the blood chemistry of rats was investigated 24 h post intravenous administration of AgNPs-CHI in comparison with the plain $AgNO_3$. Although both treatments in question did not result in a significant elevation of the hepatic function markers, AST and ALT, there was a significant impact on the renal function as evidenced by an approximately 2-fold elevation in CRE level, and 1.5-fold elevation in the serum levels of TP and Urea upon administration of $AgNO_3$. On the other hand, there was no significant impact on renal function by the administration of AgNPs-CHI (Figure 5).

Discussion

The technology of AgNPs has increasingly become important in the pharmaceutical field, either as a therapeutic modality or a drug delivery platform [8,9]. However, the concerns associated with their biosafety and lack of selectivity limit their *in vivo* applications [1,6]. Modifying the nanoparticles with targeting ligands has been extensively investigated in literature during the past two decades [24]. Nevertheless, the rapid change in the paradigm of drug delivery from basic to translational research has necessitated the simplification of the sophisticated drug delivery systems to promote their scalability and subsequently, clinical translatability [1,26]. Functional coating of nanoparticles is one of the simple and scalable approaches to tackle these challenges. Our research group has been in the process of developing and extending the applications of such an emerging technology to modulate the performance of AgNPs. In one study, we demonstrated that ethyl cellulose-coated AgNPs possess a promising performance as cytotoxic agents against breast cancer cells [29]. In another study, the PEG-coated AgNPs improved the delivery of doxorubicin to cancer cells [9]. CHI is a semi-synthetic biopolymer with diverse pharmaceutical applications [14]. Thanks to its attractive features including ease of fabrication, economic price, biotolerability, flexibility, and versatile applicability [30], we selected CHI as a model biopolymer for the functional coating of AgNPs and investigated its impact on their *in vivo* biodistribution and biosafety post intravenous administration to rats. A fast one-pot reaction based on the $NaBH_4$-mediated reduction of $AgNO_3$ precursor in the presence of CHI was used for the simultaneous preparation and coating of AgNPs (Figure 1). Previous reports revealed that the process of AgNPs-CHI formation is mediated through two major steps: adsorption of silver ions onto amino groups in CHI, and the subsequent reduction of silver ions into CHI-coated metallic silver [31]. The proposed mechanism is schemed in Figure 6. First, the silver ions from the precursor solution ($AgNO_3$) are complexed with amino groups in CHI with a high binding affinity, either through sharing the lone electron pair on the nitrogen atoms with the silver ions or through the competitive exchange of protons from the protonated amino groups in the acidic medium with silver ions in the solution. Subsequently, the silver ion-CHI complexes ($R–NH_2Ag^+$) are subjected to a second competitive exchange with water molecules in the solution, arising from the greater binding affinity of silver ions with hydroxyl groups in water owing to the superior electronegativity of oxygen atoms compared to nitrogen atoms. The latter reaction leads to the formation of silver hydroxide (Figure 6(A)). In the second step, silver hydroxide hydrolyzes rapidly in the aqueous solution, with the final formation of silver oxide. The silver oxide molecules are then reduced by the multiple alcohol moieties in the CHI, in addition to the reducing power of $NaBH_4$, with the deposition of the reduced metallic silver and the oxidation of the alcohol groups into the corresponding aldehydes (for primary alcohol groups), ketones (for secondary alcohol groups), and finally carboxylic acids (Figure 6(B)) [32,33]. The CHI-bound metallic silver is subsequently deposited in the form of nanoparticles that can be retrieved by centrifugation [34].

The formation of AgNPs-CHI was confirmed by UV-VIS spectroscopy. The presence of one absorption band also delineates the formation of spherical nanoparticles [35]. In addition, the successful formation of AgNPs-CHI was demonstrated from the observed lower peak intensity of coated AgNPs (AgNPs-CHI) compared with the uncoated nanosilver, as reported previously [9]. Moreover, DLS studies revealed the superiority of medium molecular weight CHI-coated AgNPs compared to those coated with low molecular weight CHI. The large hydrodynamic diameters (>600 nm) and low zeta potential (<10 mV) of low molecular weight CHI-coated AgNPs suggested poor stability of the developed nanosystems, inefficient coating, and a low possibility for *in vivo* applications. This comes in agreement with some previous studies which

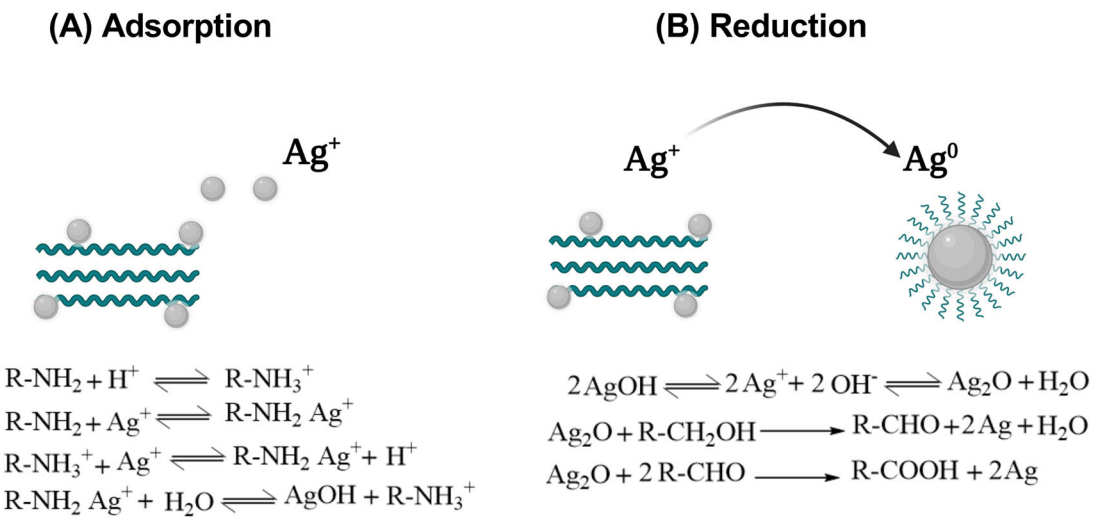

Figure 6. A proposed mechanism for the formation of AgNPs-CHI. (A) Adsorption of silver ions onto the amino groups in chitosan. (B) Reduction of silver ions into metallic nanosilver by the alcohol groups in chitosan, which are subsequently oxidized into the corresponding carbonyl groups and carboxylic acids. The symbol (R) in equations refers to the remaining structure of chitosan other than the functional groups that participate into the reactions.

pointed to the low spreadability of the low molecular weight CHI, thus limiting its coating performance [36,37]. On the other hand, the moderate particle size and high zeta potential of medium molecular weight CHI-coated AgNPs suggested an efficient coating. It has been reported that the particle size of AgNPs exerts a substantial impact on their *in vivo* performance. Ultra-fine AgNPs possess a massive surface area that increases the risks of toxicity, immunogenicity, and interactions with plasma proteins [38,39]. Meanwhile, aggregated AgNPs have been associated with poor tissue penetration, excessive phagocytosis, and low biological activity [40]. Accordingly, AgNPs with a particle diameter in the range of 150–300 nm may be optimum for *in vivo* applications. Therefore, medium molecular weight CHI-coated AgNPs were selected for the subsequent experiments, where the resultant nanoparticles were referred to as AgNPs-CHI. Previous studies pointed to the pivotal dual role of polymers as potent reducing agents and stabilizers of AgNPs. Abdellatif and coworkers recruited PVP as a stabilizing agent for AgNPs [41]. In another study, our group reported similar findings upon using various cellulosic polymers including methyl cellulose (MC), ethyl cellulose (EC), and hydroxypropyl methyl cellulose (HPMC) as stabilizers for AgNPs [11]. Herein, we propose that the medium molecular weight CHI acted both as a reducing agent and a stabilizer that improved the colloidal stability of AgNPs-CHI. In addition, the highly-positive zeta potential of the resultant particles exerted high repulsive forces that minimized their aggregation tendency, unlike AgNPs that were coated with a low molecular weight CHI that resulted in a low zeta potential with a higher aggregation tendency. In a recent study, we confirmed that AgNPs-CHI retained their stability and physico-chemical properties up to 2 months upon storage either at room temperature or 4 °C [34]. It is noteworthy that TEM examination of AgNPs-CHI revealed a spherical morphology with an average diameter of ~20 nm. The discrepancy between the particle size values obtained from DLS and TEM can be understood in lights of the difference between the adopted techniques, where DLS measurements usually reveal the hydrodynamic diameter of the whole colloidal particles. On the other hand, TEM likely visualizes the metallic core of the metallic nanoparticles, as reported previously [42]. Furthermore, the dehydration that is usually associated with the preparation of TEM samples usually results in smaller particle size values in comparison with the fully-hydrated environment in the case of DLS [43,44].

Sprague–Dawley rats were recruited as a representative animal model for our *in vivo* study. This model has been chosen as the most preferred model for studies on AgNPs according to a huge number of studies, thanks to its close resemblance to the human anatomy, ease of breeding and handling, moderate organ size for analytical applications, and the sufficient blood volume that enables adequate serum analysis [45–48]. The *in vivo* biodistribution studies revealed a limited capability of clearing the plain silver from the systemic circulation by the major organs, including the liver which cleared only about 20% of the silver amount. This comes in agreement with the findings of previous studies [49–51]. On the other hand, functional coating with CHI resulted in a nearly-complete clearance of silver from the systemic circulation, with a dramatic increase in its hepatic accumulation by more than 3 folds. This may be attributed to the highly-positive surface charge of CHI which can promote its interaction with the anionic heparan sulfate proteoglycans (HSPGs) that are overexpressed onto the surfaces of hepatocytes [22,52]. In addition, the carbohydrate nature of CHI might have promoted its affinity to the liver and the subsequent uptake by hepatocytes thanks to the high physiological capability of the liver for carbohydrate metabolism [53,54]. Moreover, a recent report revealed the increased cellular uptake of CHI-coated nanoparticles *via* both clathrin-mediated endocytosis and macropinocytosis in contrary to most nanomedicines that are mainly taken up *via* the clathrin-mediated pathway [55]. It has also been reported that the non-classical pathway of macropinocytosis is less-destructive for nanomedicines compared to the classical clathrin-mediated pathway that mostly ends up with a substantial lysosomal degradation [6,56]. Furthermore, several studies reported on the increased permeation and transcellular transport of CHI-coated nanomedicines owing to the ability of CHI to increase the fluidity of cellular membrane lipids and induce a redistribution of membrane proteins [57–59]. Meanwhile, the functional coating of AgNPs with CHI reduced its renal biodistribution by 2 folds, suggesting that CHI-coated nanosilver is mainly cleared through the liver with limited accessibility to the kidneys.

The serum analysis of rats suggested a significant impairment of renal function by the administration of plain silver in comparison with AgNPs-CHI. This can be understood in terms of the limited renal exposure to the administered AgNPs-CHI, while the

animals that received $AgNO_3$ had a 2-fold higher renal levels of Ag, as shown by the biodistribution findings alluded to above. Several toxicological reports have pointed to the toxic effects of silver on the kidneys, which are manifested by an increased rate of cellular apoptosis, Tumor Necrosis Factor-alpha (TNF-α) and Transforming Growth Factor Beta (TGFβ)-mediated inflammation, and dehydration [10,60]. Our findings presented in this study suggest that coating the nanosilver with CHI can minimize renal exposure to the silver and the subsequent nephrotoxicity. In addition, the elevation of TP in serum post administration of $AgNO_3$ is a marked sign of systemic inflammation [61], which could not be observed in the case of AgNPs-CHI that seemed to be well-tolerated by the body with a semi-complete clearance from the systemic circulation as shown above.

The findings of the present study revealed that coating AgNPs with CHI can modulate their biodistribution, selectivity, clearance, and biosafety following systemic administration. Therefore, such a simple and scalable approach can expand the *in vivo* applications of AgNPs as liver-targeting drug delivery carriers that will be beneficial in the treatment of various liver disorders or cancers. In addition, the novel platform presented here can be invested for the delivery of diagnostic elements to the liver. The functional coating of AgNPs with biopolymers seems to be a promising strategy to substitute the classic ligand-based active targeting that is limited in terms of stability, scalability, and clinical translatability. However, our strategy has some important limitations that should be carefully considered. First, the selection of the polymer to be used, which requires well-established studies on its physico-chemical properties, stability, compatibility with AgNPs, and biosafety. Second, the selection of a proper coating technique that should be simple, fast, compatible with the reaction medium, feasible, and applicable on a large scale. Third, the behavior of the coating material (e.g. spreadability) is a critical factor in determining the efficiency of the coating and the physico-chemical properties of the resultant AgNPs, as can be concluded from our comparative results between the low molecular weight CHI versus its medium molecular weight counterpart. We believe that further research in this direction will promote the clinical translation of AgNPs and expand their applicability beyond the current well-established topical applications.

Conclusions

We investigated the impact of coating AgNPs with CHI on their *in vivo* performance and biosafety following intravenous administration. Medium molecular weight CHI resulted in an efficient and stable coating compared to its low molecular weight counterpart. AgNPs-CHI demonstrated a high *in vivo* tolerability with a semi-complete clearance from the systemic circulation and a liver-dominant tissue tropism. On the other hand, plain $AgNO_3$ demonstrated poor clearance from systemic circulation, high renal exposure, and nonspecific tissue accumulation. Serological examinations revealed the normal level of hepato-renal function markers post administration of AgNPs-CHI, in contrary with $AgNO_3$ that resulted in a significant elevation of CRE, Urea, and TP, which reflects nephrotoxicity and inflammation. It can be concluded that the functional coating of AgNPs with CHI promotes their bio tolerability and hepatic selectivity which can be invested in the development of highly-biosafe nanocarriers for the treatment of liver diseases.

Acknowledgement

The authors would like to thank the Department of Industrial Pharmacy, Faculty of Pharmacy, Assiut University for supporting this study.

Disclosure statement

No potential conflict of interest was reported by the author(s).

Funding

The author(s) reported there is no funding associated with the work featured in this article.

ORCID

Hesham M. Tawfeek http://orcid.org/0000-0001-9789-9953
Mahmoud A. Younis http://orcid.org/0000-0001-9722-3267

References

[1] Younis MA, Tawfeek HM, Abdellatif AAH, et al. Clinical translation of nanomedicines: challenges, opportunities, and keys. Adv Drug Deliv Rev. 2022;181:114083.
[2] Younis MA, Khalil IA, Harashima H. Gene therapy for hepatocellular carcinoma: highlighting the journey from theory to clinical applications. Adv Therap. 2020;3(11):2000087.
[3] Khalil IA, Younis MA, Kimura S, et al. Lipid nanoparticles for cell-specific in vivo targeted delivery of nucleic acids. Biol Pharm Bull. 2020;43(4):584–595.
[4] Nakamura T, Sato Y, Yamada Y, et al. Extrahepatic targeting of lipid nanoparticles in vivo with intracellular targeting for future nanomedicines. Adv Drug Deliv Rev. 2022;188:114417.
[5] Abdellatif AAH, Younis MA, Alsowinea AF, et al. Lipid nanoparticles technology in vaccines: shaping the future of prophylactic medicine. Colloids Surf B Biointerfaces. 2023;222:113111.
[6] Abdellatif AAH, Younis MA, Alsharidah M, et al. Biomedical applications of quantum dots: overview, challenges, and clinical potential. Int J Nanomedicine. 2022;17:1951–1970.
[7] Abdellatif A, Osman S, Alsharidah M, et al. Green synthesis of silver nanoparticles reduced with Trigonella foenum-graecum and their effect on tumor necrosis factor-α in MCF7 cells. Eur Rev Med Pharmacol Sci. 2022;26(15):5529–5539.
[8] Abdellatif AAH, Alhathloul SS, Aljohani ASM, et al. Green synthesis of silver nanoparticles incorporated aromatherapies utilized for their antioxidant and antimicrobial activities against some clinical bacterial isolates. Bioinorg Chem Appl. 2022;2022:2432758.
[9] Abdelfattah A, Aboutaleb AE, Abdel-Aal ABM, et al. Design and optimization of PEGylated silver nanoparticles for efficient delivery of doxorubicin to cancer cells. J Drug Delivery Sci Technol. 2022;71:103347.
[10] Drake PL, Hazelwood KJ. Exposure-related health effects of silver and silver compounds: a review. Ann Occup Hyg. 2005;49(7):575–585.
[11] Abdellatif AAH, Alturki HNH, Tawfeek HM. Different cellulosic polymers for synthesizing silver nanoparticles

with antioxidant and antibacterial activities. Sci Rep. 2021; 11(1):84.
[12] Xiang S, Ma X, Shi H, et al. Green synthesis of an alginate-coated silver nanoparticle shows high antifungal activity by enhancing its cell membrane penetrating ability. ACS Appl Bio Mater. 2019;2(9):4087–4096.
[13] Carotenuto G. Synthesis and characterization of poly(N-vinylpyrrolidone) filled by monodispersed silver clusters with controlled size. Appl Organometal Chem. 2001;15(5): 344–351.
[14] Jiménez-Gómez CP, Cecilia JA. Chitosan: a natural biopolymer with a wide and varied range of applications. Molecules. 2020;25(17):3981.
[15] Salatin S, Yari Khosroushahi A. Overviews on the cellular uptake mechanism of polysaccharide colloidal nanoparticles. J Cell Mol Med. 2017;21(9):1668–1686.
[16] Xia W, Liu P, Zhang J, et al. Biological activities of chitosan and chitooligosaccharides. Food Hydrocoll. 2011;25(2): 170–179.
[17] Nam K-S, Choi Y-R, Shon Y-H. Evaluation of the antimutagenic potential of chitosan oligosaccharide: Rec, Ames and Umu tests. Biotechnol Lett. 2001;23(12):971–975.
[18] May KL, Tangso KJ, Hawley A, et al. Interaction of chitosan-based dietary supplements with fats during lipid digestion. Food Hydrocoll. 2020;108:105965.
[19] Mi F-L, Wu S-J, Zhong W-Q, et al. Preparation of a silver nanoparticle-based dual-functional sensor using a complexation–reduction method . Phys Chem Chem Phys. 2015; 17(33):21243–21253.
[20] Atia NN, Tawfeek HM, Rageh AH, et al. Novel sublingual tablets of atorvastatin calcium/trimetazidine hydrochloride combination; HPTLC quantification, in vitro formulation and characterization. Saudi Pharm J. 2019;27(4):540–549.
[21] Younis MA, Khalil IA, Elewa YHA, et al. Ultra-small lipid nanoparticles encapsulating sorafenib and midkine-siRNA selectively-eradicate sorafenib-resistant hepatocellular carcinoma in vivo. J Control Release. 2021;331:335–349.
[22] Younis MA, Khalil IA, Abd Elwakil MM, et al. A multifunctional lipid-based nanodevice for the highly specific codelivery of sorafenib and midkine siRNA to hepatic cancer cells. Mol Pharm. 2019;16(9):4031–4044.
[23] Shomer NH, Allen-Worthington KH, Hickman DL, et al. Review of rodent euthanasia methods. J Am Assoc Lab Anim Sci. 2020;59(3):242–253.
[24] Abdellatif AAH, Khan RA, Alhowail AH, et al. Octreotide-conjugated silver nanoparticles for active targeting of somatostatin receptors and their application in a nebulized rat model. Nanotechnol Rev. 2021;11(1):266–283.
[25] Lee RF, Pickering WF. Effect of precipitate and complex formation on the determination of silver by atomic-absorption spectroscopy. Talanta. 1971;18(11):1083–1094.
[26] Younis MA, Sato Y, Elewa YHA, et al. Self-homing nanocarriers for mRNA delivery to the activated hepatic stellate cells in liver fibrosis. J Control Release. 2023;353:685–698.
[27] Aboutaleb AE, Abdel-Rahman SI, Mo A, et al. Design and evaluation of domperidone sublingual tablets. Int J Pharm Pharm Sci. 2016;8(6):195–201.
[28] Smith PK, Krohn RI, Hermanson GT, et al. Measurement of protein using bicinchoninic acid. Anal Biochem. 1985; 150(1):76–85.
[29] Abdellatif AAH, Alsharidah M, Al Rugaie O, et al. Silver nanoparticle-coated ethyl cellulose inhibits tumor necrosis factor-α of breast cancer cells. Drug Des Devel Ther. 2021; 15:2035–2046.
[30] Zhao D, Yu S, Sun B, et al. Biomedical applications of chitosan and its derivative nanoparticles. Polymers. 2018;10(4): 462.
[31] Kulikouskaya V, Hileuskaya K, Kraskouski A, et al. Chitosan-capped silver nanoparticles: a comprehensive study of polymer molecular weight effect on the reaction kinetic, physicochemical properties, and synergetic antibacterial potential. SPE Polym. 2022;3(2):77–90.
[32] Wei D, Ye Y, Jia X, et al. Chitosan as an active support for assembly of metal nanoparticles and application of the resultant bioconjugates in catalysis. Carbohydr Res. 2010; 345(1):74–81.
[33] Carapeto AP, Ferraria AM, do Rego AMB. Unraveling the reaction mechanism of silver ions reduction by chitosan from so far neglected spectroscopic features. Carbohydr Polym. 2017;174:601–609.
[34] Abdellatif AAH, Abdelfattah A, Younis MA, et al. Chitosan-capped silver nanoparticles with potent and selective intrinsic activity against the breast cancer cells. Nanotechnology Reviews. 2023;12(1):20220546.
[35] Mulfinger L, Solomon SD, Bahadory M, et al. Synthesis and study of silver nanoparticles. J Chem Educ. 2007;84(2):322.
[36] Kouchak M, Avadi M, Abbaspour M, et al. Effect of different molecular weights of chitosan on preparation and characterization of insulin loaded nanoparticles by ion gelation method. Intl J Drug Dev Res. 2012;4(2):271–277.
[37] Kapadnis G, Dey A, Dandekar P, et al. Effect of degree of deacetylation on solubility of low-molecular-weight chitosan produced via enzymatic breakdown of chitosan. Polym Int. 2019;68(6):1054–1063.
[38] Cho YM, Mizuta Y, Akagi JI, et al. Size-dependent acute toxicity of silver nanoparticles in mice. J Toxicol Pathol. 2018; 31(1):73–80.
[39] Stensberg MC, Wei Q, McLamore ES, et al. Toxicological studies on silver nanoparticles: challenges and opportunities in assessment, monitoring and imaging. Nanomedicine. 2011;6(5):879–898.
[40] Bélteky P, Rónavári A, Zakupszky D, et al. Are smaller nanoparticles always better? Understanding the biological effect of size-dependent silver nanoparticle aggregation under biorelevant conditions. Int J Nanomedicine. 2021;16:3021–3040.
[41] Abdellatif AAH, Abdelfattah A, Bouazzaoui A, et al. Silver nanoparticles stabilized by poly (vinyl pyrrolidone) with potential anticancer activity towards prostate cancer. Bioinorg Chem Appl. 2022;2022:6181448.
[42] Fissan H, Ristig S, Kaminski H, et al. Comparison of different characterization methods for nanoparticle dispersions before and after aerosolization. Anal Methods. 2014;6(18): 7324–7334.
[43] Mourdikoudis S, Pallares RM, Thanh NTK. Characterization techniques for nanoparticles: comparison and complementarity upon studying nanoparticle properties. Nanoscale. 2018;10(27):12871–12934.
[44] Michen B, Geers C, Vanhecke D, et al. Avoiding drying-artifacts in transmission electron microscopy: characterizing the size and colloidal state of nanoparticles. Sci Rep. 2015; 5(1):9793.
[45] Ebabe Elle R, Gaillet S, Vidé J, et al. Dietary exposure to silver nanoparticles in Sprague-Dawley rats: effects on

oxidative stress and inflammation. Food Chem Toxicol. 2013;60:297–301.
[46] Lee JH, Kim YS, Song KS, et al. Biopersistence of silver nanoparticles in tissues from Sprague-Dawley rats. Part Fibre Toxicol. 2013;10:36.
[47] Sung JH, Ji JH, Yoon JU, et al. Lung function changes in Sprague-Dawley rats after prolonged inhalation exposure to silver nanoparticles. Inhal Toxicol. 2008;20(6):567–574.
[48] Nahas K, Provost JP, Baneux PH, et al. Effects of acute blood removal via the sublingual vein on haematological and clinical parameters in Sprague-Dawley rats. Lab Anim. 2000;34(4):362–371.
[49] Fennell TR, Mortensen NP, Black SR, et al. Disposition of intravenously or orally administered silver nanoparticles in pregnant rats and the effect on the biochemical profile in urine. J Appl Toxicol. 2017;37(5):530–544.
[50] Lansdown ABG. A pharmacological and toxicological profile of silver as an antimicrobial agent in medical devices. Adv Pharmacol Sci. 2010;2010:910686.
[51] Walker M, Parsons D. The biological fate of silver ions following the use of silver-containing wound care products - a review. Int Wound J. 2014;11(5):496–504.
[52] Roskams T, Moshage H, De Vos R, et al. Heparan sulfate proteoglycan expression in normal human liver. Hepatology. 1995;21(4):950–958.
[53] Jiang LQ, Wang TY, Wang Y, et al. Co-disposition of chitosan nanoparticles by multi types of hepatic cells and their subsequent biological elimination: the mechanism and kinetic studies at the cellular and animal levels. Int J Nanomed. 2019;14:6035–6060.
[54] Loh JW, Yeoh G, Saunders M, et al. Uptake and cytotoxicity of chitosan nanoparticles in human liver cells. Toxicol Appl Pharmacol. 2010;249(2):148–157.
[55] Dou T, Wang J, Han C, et al. Cellular uptake and transport characteristics of chitosan modified nanoparticles in caco-2 cell monolayers. Int J Biol Macromol. 2019;138:791–799.
[56] Khalil IA, Kogure K, Akita H, et al. Uptake pathways and subsequent intracellular trafficking in nonviral gene delivery. Pharmacol Rev. 2006;58(1):32–45.
[57] Bruinsmann FA, Pigana S, Aguirre T, et al. Chitosan-Coated nanoparticles: effect of chitosan molecular weight on nasal transmucosal delivery. Pharmaceutics. 2019;11(2):86.
[58] Alalaiwe A, Carpinone P, Alshahrani S, et al. Influence of chitosan coating on the oral bioavailability of gold nanoparticles in rats. Saudi Pharm J. 2019;27(2):171–175.
[59] Zheng A-P, Liu H-X, Yuan L, et al. Comprehensive studies on the interactions between chitosan nanoparticles and some live cells. J Nanopart Res. 2011;13(10):4765–4776.
[60] Nosrati H, Hamzepoor M, Sohrabi M, et al. The potential renal toxicity of silver nanoparticles after repeated oral exposure and its underlying mechanisms. BMC Nephrol. 2021;22(1):228.
[61] Kaysen GA. Effects of inflammation on plasma composition and endothelial structure and function. J Ren Nutr. 2005; 15(1):94–98.